

ACCURACY-IMPROVEMENT SIMULATION OF SELF-MIXING SEMICONDUCTOR LASER RANGE FINDER DRIVEN BY RESHAPED MODULATION CURRENT

Shigenobu Shinohara, Kazuhiko Nobunaga, Hirofumi Yoshida,
Hiroaki Ikeda, Masafumi Miyata*, Ken-ichi Nishide*
and Masao Sumi**

Shizuoka University, Hamamatsu, 432 JAPAN

* Tokyo Aircraft Instrument Co. Ltd., Komae, 201 JAPAN

** Chiba Institute of Technology, Narashino, 275 JAPAN

ABSTRACT

Accuracy improvement of a self-mixing semiconductor laser range finder is predicted by simulation, in which the laser modulation current is reshaped to give an ideal triangular waveform of the optical frequency change. The maximum range measurement error of less than 0.1% in a wide range of 0.1m to 1m is expected by the reshaping of the modulation current.

Experimental verification of the effect of current reshaping on the linearization of the derivative of the optical frequency change curve is given.

1. INTRODUCTION

Compact and high-accuracy ($\pm 0.5\%$) range finder utilizing a self-mixing semiconductor laser has been demonstrated by the authors.(1),(2) The range finder can measure a short distance from the laser diode (LD) to a target positioned in a range of 0.2m to 1m using only one sensing head. In order to further improve the accuracy it is required to linearize the optical frequency change during the half period of the FM modulation so as to give an ideal triangular waveform of the optical frequency change.

Therefore, in this paper, simulation of reshaping the modulation current is performed to get optimal conditions for an ideal triangular optical frequency change. And range measurement error due to the residual distortion of the optical frequency change is calculated as functions of reshaping conditions. The effect of the waveform reshaping on the linearization is confirmed by an experiment.

2. PRINCIPLE OF MEASUREMENT

The Principle and method of range measure-

ment is shown in Fig.1. The signal (a) from a photodiode (PD) accommodated in the LD package has stair-like discontinuities, which are introduced by the mode hops. The mode-hop interval (MHI) differs slightly from each other owing to both the laser FM noise and the time dependent FM modulation efficiency. The range L_T to the target is given by the following equations,

$$L_T = cT/4i_m \Delta F_e T_M \quad (1)$$

$$1/T_M = (N_1/T_1 + N_2/T_2)/2 \quad (2)$$

where c is the light velocity, T the period of the triangular wave current, i_m the peak-to-peak amplitude of the current, ΔF_e the effective FM modulation efficiency and T_M the mean value of the $N_1 + N_2$ MHI's.

Measurement error due to the FM noise has been reduced by averaging several hundreds of MHI's(1). The error caused by the phase change of returned light reflected from a focusing lens

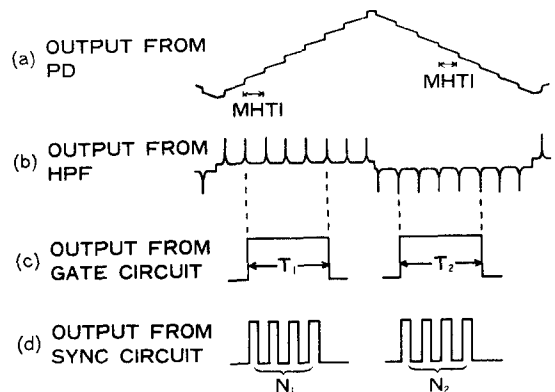


Fig.1 Principle and method of range measurement.

has been reduced by stabilizing the temperature of the lens holder⁽²⁾. When the amount of reflection from the focusing lens is so small as the feedback parameter is $\xi_L \approx 0.02$, the sinusoidal-wave like fluctuation in the FM modulation efficiency curve during the half modulation period becomes negligible⁽³⁾. Then the FM modulation efficiency curve approaches a monotonously increasing curve as shown in Fig.2.

In such a case, the measurement error due to the unavoidable change of both the position and the width of the measuring gate pulse will be estimated as the variation of the normalized modulation efficiency $\Delta F(t)$ during the maximum gate shift of $T_M/2$. For example, in case of the revised range finder (see Fig.3 and Fig.6 in reference (2)) an estimated maximum error is $\pm 3.7\text{mm}$, which agrees well with the observed maximum error $\pm 2.8\text{mm}$. Therefore the error due to the gate shift will be greatly reduced by maintaining the FM modulation efficiency, (or more precisely, the derivative of the optical frequency change curve) constant. One of the means to linearize the optical frequency change is to reshape the modulation current.

3. SIMULATION

Current Reshaping: The modulation current is reshaped by summing both a triangular wave and an integrated wave of rectangle. First, the triangular waveform $g(t)$ shown in Fig.3 is described as follows:

$$g(t) = V_m t / t_1, \quad (0 \leq t \leq t_1) \quad (3)$$

$$g(t) = V_m (2 - t / t_1), \quad (t_1 \leq t \leq 2t_1) \quad (4)$$

Then the $g(t)$ is expanded by Fourier series as

$$g(t) = V_m / 2 - (4V_m / \pi^2) \sum_{m=1}^{\infty} (1 / (2m-1)^2) \cdot \cos(2m-1)\omega t \quad (5)$$

$$\omega = \pi / t_1 \quad (6)$$

where V_m is the amplitude of the triangular wave, ω the angular frequency and t_1 the half of the period.

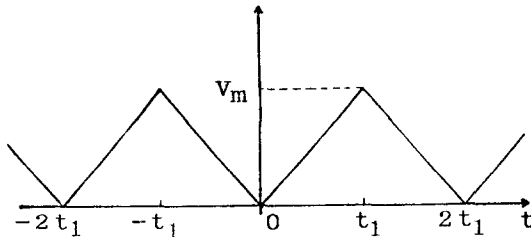


Fig.3 Triangular voltage waveform to form a reshaped modulation current.

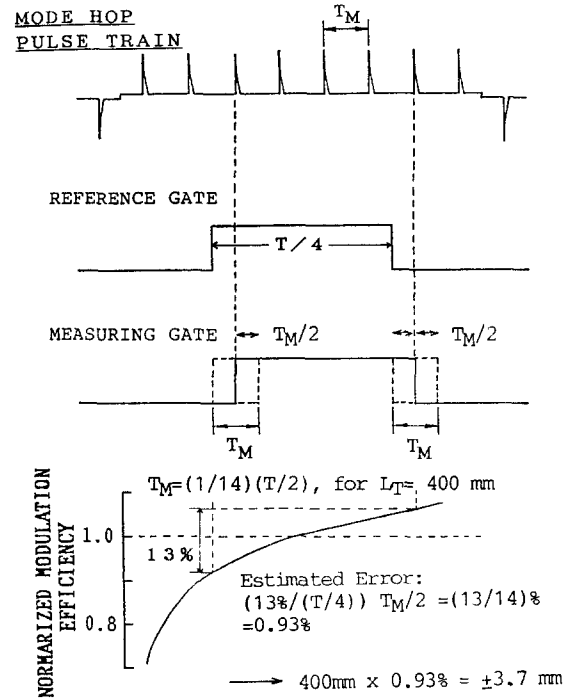


Fig.2 The shift of the measuring gate pulse due to the target, and its influence on measurement error.

Integrated waveform of rectangle: A rectangular wave with both a zero-to-peak amplitude of E and the period of $2t_1$ is integrated using a C-R integration circuit. The integration circuit for charging and discharging is shown by (a) and (b) in Fig.4, respectively. In stationary state, the integrated waveform $V_C(t)$ becomes a distorted triangular waveform as shown in Fig.5, where the initial voltage E_I and the final voltage E_F of the charged capacitor are shown. The E_I and E_F are given by

$$E_I = E \exp(-t_1 / RC) / [1 + \exp(-t_1 / RC)] \quad (7)$$

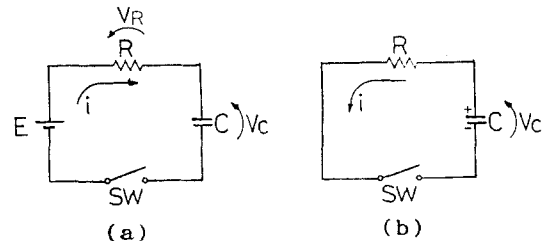


Fig.4 Circuit configuration for (a) charging and (b) discharging a capacitor in the C-R integrator.

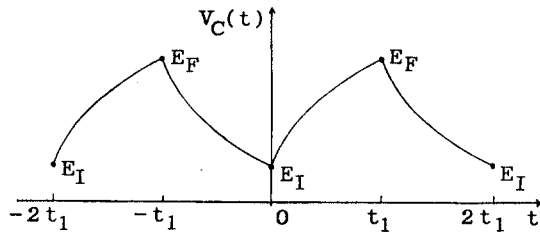


Fig.5 The composite voltage waveform.

$$E_F = E / [1 + \exp(-t_1/RC)] \quad (8)$$

The waveform $V_C(t)$ is described as

$$V_C(t) = E \exp[-(t+t_1)/RC] / [1 + \exp(-t_1/RC)], \quad (-t_1 \leq t \leq 0) \quad (9)$$

$$V_C(t) = E - E \exp(-t/RC) / [1 + \exp(-t_1/RC)], \quad (0 \leq t \leq t_1) \quad (10)$$

Then the $v_C(t)$ is transformed into a Fourier series as

$$V_C(t) = E/2 - (2E/t_1) \sum_{n=1}^{\infty} [G \cos(n\omega t) + H \sin(n\omega t)] \quad (11)$$

$$n = 2m-1, (m=1, 2, 3, \dots) \quad (12)$$

where G and H are given by

$$G = (1/RC) / [(-1/RC)^2 + n^2\omega^2] \quad (13)$$

$$H = n\omega / [(-1/RC)^2 + n^2\omega^2] - 1/n\omega \quad (14)$$

Calculation of Composite Wave: The composite waveform of the summed voltage $V(t)$ is given by

$$V(t) = g(t) + V_C(t) = V_m/2 + E/2 - 2 \sum_{n=1}^{\infty} K_n \sin(n\omega t + \psi_n) \quad (15)$$

where K_n and ψ_n are the amplitude and the phase of the n th harmonic of the fundamental wave of the composite wave, and given as follows:

$$K_n = (1/a^2b) [a^2E^2t_1^4 + (2V_m b + a^2Et_1RC)^2]^{1/2} \quad (16)$$

$$\psi_n = \cos^{-1} [-aEt_1^2 / [a^2E^2t_1^4 + (2V_m b + a^2Et_1RC)^2]^{1/2}] \\ = \sin^{-1} (2V_m b + a^2Et_1RC) / [a^2E^2t_1^4 + (2V_m b + a^2Et_1RC)^2]^{1/2} \quad (17)$$

and where

$$\left. \begin{aligned} a &= (2m-1)\pi \\ b &= t_1^2 + (2m-1)^2\pi^2 R^2 C^2 \\ A &= -Et_1^2/ab \\ B &= (2V_m b + a^2Et_1RC)/a^2b. \end{aligned} \right\} \quad (18)$$

Consequently, the drive current $i(t)$ of the laser diode is given by

$$i(t) = V(t)/Z \quad (19)$$

where Z denotes the sum of the differential resistance of the LD and a current monitor resistance.

On the other hand, when an LD is frequency modulated with a sinusoidal current $I_n \sin(n\omega t)$ the optical frequency change is given by $A_n I_n \sin(n\omega t + \phi_n)$. Where $n\omega$ is the angular frequency, n the integer, ω the fundamental angular frequency of the triangular wave, I_n the amplitude, A_n the FM efficiency at a frequency of the n th harmonic and $-\phi_n$ the phase angle by which an optically discriminated sinusoidal wave lags the inverted sinusoidal modulating current. Consequently, using the Fourier series in eqs. (18) and (19) the optical frequency $f(t)$ of an LD is given by

$$f(t) = f_{00} - (2/Z) \sum_{n=1}^{\infty} A_n K_n \sin(n\omega t + \psi_n + \phi_n) \quad (20)$$

$$n = 2m-1, m = 1, 2, 3, \dots \quad (21)$$

where f_{00} is the constant free-running frequency without modulation and optical feedback.

Laser Diode Used for Calculation: The FM modulation characteristics of a laser diode used for calculation is described below

$$A_n = A_1 (1 - 0.16 \log_{10} n), \quad [\text{GHz/mA}] \quad (22)$$

$$\phi_n = -(\pi/180) (5.2 + 3.05 \log_{10} n), \quad [\text{rad}] \quad (23)$$

$$n = 2m-1, m = 1, 2, 3, \dots 50 \quad (24)$$

where $A_1 (=3.81 \text{ GHz/mA})$ is the frequency deviation per unit current amplitude when the laser is sinusoidally modulated at a frequency of 0.5 kHz, which is a fundamental frequency of the triangular current. Those values of A_n and ϕ_n in eqs. (22)-(24) are quoted from reference (3), however, the values depend on a used LD.

Waveform Reshaping Circuit: Figure 6 shows the block diagram of the waveform-reshaping circuit for the FM modulation of a laser diode.

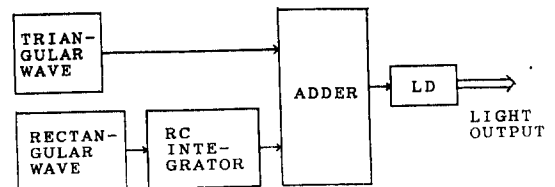


Fig.6 Block diagram of the waveform-reshaping circuit for the FM modulation of a laser diode.

The parameters are a time constant of the RC integrator and an amplitude ratio of the triangular wave to the integrated wave. The parameters are so chosen that the optical frequency change during both the ascending and descending half period becomes as linear as possible.

4. SIMULATION RESULTS

Figure 7 shows an example of reshaped modulation current waveform, which are composed of both a triangular wave and an integrated wave. The reshaped current waveform is obtained under a nearly optimal condition that the time constant

for integration is 0.163ms and the amplitude ratio is 13.0. Note that the ordinate scale for the integrated curve (middle) is expanded. The feature of the composite current waveform is that the current during the ascending half period has a smooth convex near the bottom, while the current during the descending half period has a smooth concave near the top.

Figure 8 shows a simulation result of normalized distortion of optical frequency with reference to an ideal triangular wave-form. The real and dashed curves represent the normalized distortions obtained by reshaping and preceding methods, respectively. The real curve is obtained using the composite wave shown in Fig.7. The maximum normalized distortion of -4% obtained by the preceding method is greatly reduced to -0.6% by using the current reshaping method.

Figure 9 shows the diagram of theoretical equi-error lines calculated for range measurement as functions of both the time constant and the amplitude ratio of triangular wave to integrated

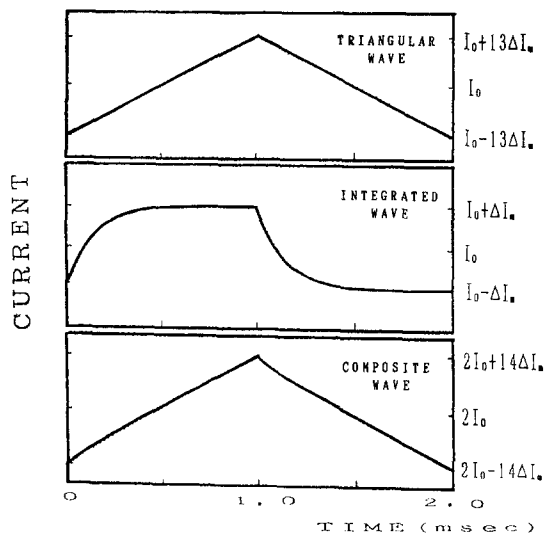


Fig.7 Reshaped modulation current waveform composed of both a triangular and an integrated waves. The time constant for integration is 0.163ms and the amplitude ratio is 13.0.

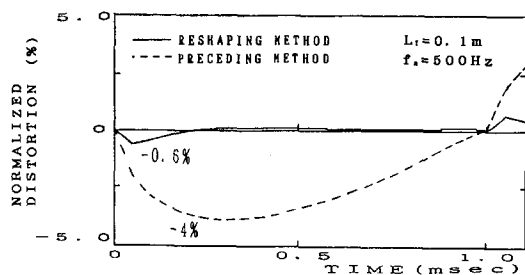


Fig.8 Simulation result of normalized distortion of optical frequency with reference to an ideal triangular waveform during a half period. The real and dashed curves represent the normalized distortions obtained by reshaping and preceding methods, respectively.

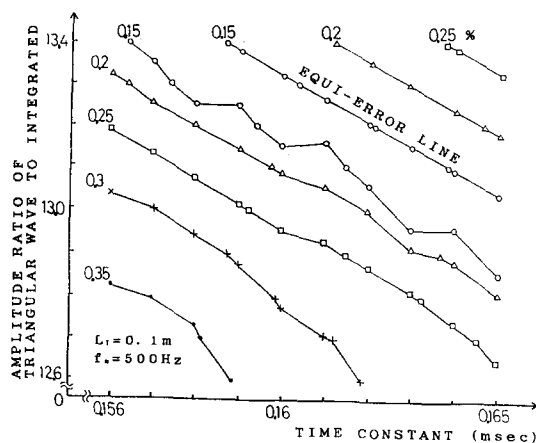


Fig.9 Diagram of theoretical equi-error lines calculated for range measurement as functions of both the time constant and the amplitude ratio of triangular wave to integrated wave. The parameter is a measurement error in percent. Range is $L_T = 0.1m$.

wave. The calculated error is a maximum which is estimated for the worst case of the shortest range $L_T = 0.1m$. The maximum error will be reduced to about a tenth times of it shown in Fig.9 by averaging a hundred data. According to Fig.9 the associated parameters of time constant and amplitude ratio are distributed in a belt zone, where the error is less than a definite value. Therefore in order to obtain a definite error the time constant must be decreased when the amplitude ratio is increased.

Adjustability of Parameters: The measurement error is calculated and shown in Fig.10 as a function of the amplitude ratio when the time constant τ is kept constant, $\tau = 0.163ms$. The minimum error of 0.1% is obtained at the amplitude ratio 13.0. In order to obtain error within

0.2%, the allowable adjustment error of the amplitude ratio is $\pm 1.5\%$ around 13.1, which is realizable.

Next, keeping the amplitude ratio constant 13.0, the relation between the measurement error and the time constant is shown in Fig.11. The allowable adjustment error of the time constant to obtain error within 0.2% is $\pm 1.8\%$ around 0.165msec.

5. EXPERIMENTAL RESULTS

An experimental result of linearization of the optical frequency change waveform is shown in Fig.12, which is obtained by the reshaping of the modulation current. Compared with the dashed curve for before reshaping, the real curve for after reshaping is a little elevated in the former part of the rising half, while a little hung in the falling half. The normalized derivative of optical frequency variation approaches nearly 1.0 after reshaping. The variation of the normalized derivative during the gate width is

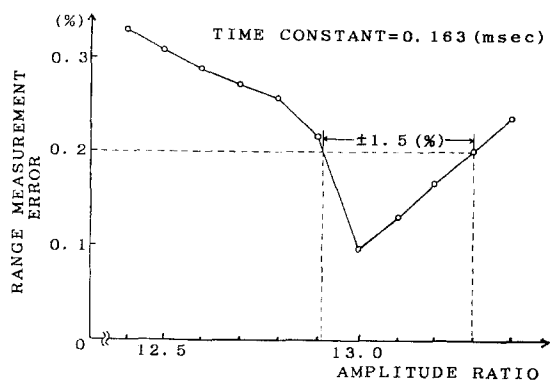


Fig.10 Range measurement error versus the amplitude ratio when the time constant is kept 0.163ms.

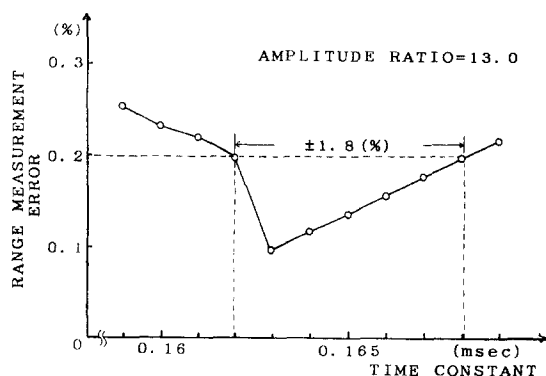


Fig.11 Range measurement error versus the time constant when the amplitude ratio is kept constant 13.0

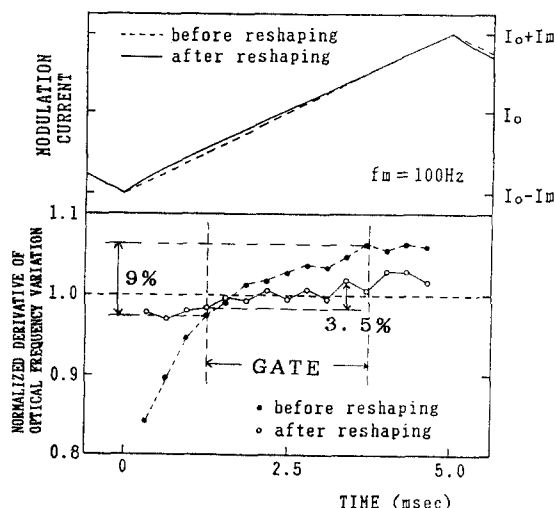


Fig.12 Experimental results of linearization of the optical frequency change waveform by the reshaping of the modulation current. The ordinate shows the normalized derivative of the optical frequency change in case of "before reshaping" and "after reshaping".

reduced from 9% to 3.5% by the reshaping. So the effect of the current reshaping on maintaining the derivative almost constant is confirmed by experiment.

The experimental verification of the accuracy improvement by the reshaping for measurement of shorter range will be published elsewhere.(4)

6. CONCLUSION

Accuracy improvement of a self-mixing semiconductor laser range finder is predicted by simulation, in which the laser modulation current is reshaped to give an ideal triangular waveform of the optical frequency change. The maximum range measurement error of less than 0.1% in a wide range of 0.1m to 1m is expected by the reshaping of the modulation current.

Experimental verification of the effect of current reshaping on the linearization of the derivative of the optical frequency change curve is given.

ACKNOWLEDGMENT

The authors wish to thank general manager Nakahama of Tokyo Aircraft Instrument Co. Ltd. for his encouragement, and Mrs. T. Sawaki for her assistance in preparing the manuscript.

REFERENCES

- (1) S.Shinohara et al., "Compact and precision range finder using self-mixing semiconductor

laser", Proceedings of '89 KACC vol.2, pp.972-978, Oct. 1989.

- (2) S.Shinohara et al., "High-resolution range finder with wide dynamic range of 0.2m to 1m using a frequency-modulated laser diode," Proceedings of IECON'89 vol.3, pp.646-651, Nov. 1989.
- (3) S.Shinohara et al., "FM-modulation distortion of light output from semiconductor laser modulated with triangular wave current", Trans. IEICE, E72, 4, pp.275-278 April 1989.
- (4) S.Shinohara et al., "High-precision range finder for slowly moving target with rough surface," to be published in Proc. of IECON'90 Nov. 1990.